AGU PUBLICATIONS

JGR

Journal of Geophysical Research: Atmospheres

RESEARCH ARTICLE
10.1002/2017JD027709

Key Points:
- Average atmospheric mixing ratios of the *i*-butane and *n*-butane and *i*-pentane and *n*-pentane isomers have been decreasing at most of the urban sites considered
- Over 15 years, the isomeric ratio of the two alkane pairs has dropped by an average of 30–45%, with a relative increase of the *n*-isomers
- Deriving national trends for mixing ratios and emission inventories from these data is impeded by the variability in results between sites

Supporting Information:
- Supporting Information S1

Correspondence to:
D. Helmig,
detlev.helmig@colorado.edu

Citation:
Rossabi, S., & Helmig, D. (2018). Changes in atmospheric butanes and pentanes and their isomeric ratios in the continental United States. *Journal of Geophysical Research: Atmospheres*, *123*, 3772–3790. https://doi.org/10.1002/2017JD027709

Received 21 SEP 2017
Accepted 18 JAN 2018
Accepted article online 13 FEB 2018
Published online 12 APR 2018

Changes in Atmospheric Butanes and Pentanes and Their Isomeric Ratios in the Continental United States

Sam Rossabi[1] **and Detlev Helmig**[1]

[1]Institute of Arctic and Alpine Research (INSTAAR), University of Colorado Boulder, Boulder, CO, USA

Abstract Nonmethane hydrocarbons have been used as tracers in research on emissions and atmospheric oxidation chemistry. This research investigates source region mixing ratio trends of the nonmethane hydrocarbons *i*-butane, *n*-butane, *i*-pentane, and *n*-pentane, and the (*i*/*n*) isomeric ratios of these compounds between 2001 and 2015. Data collected at Photochemical Assessment Monitoring Stations, mandated by the U.S. Environmental Protection Agency in ozone nonattainment areas, and data collected at Global Greenhouse Gas Reference Network sites within the National Oceanic and Atmospheric Administration network, and analyzed at the Institute of Arctic and Alpine Research at the University of Colorado-Boulder, were examined. Among all considered species, linear regression analyses on concentration time series had negative slopes at 81% of sites, indicating predominantly declining butane and pentane atmospheric concentrations. Mostly negative slopes (78% of sites) were found for the (*i*/*n*) butane and pentane isomeric ratios, including all six and seven statistically significant (*i*/*n*) butane and pentane trends, respectively. Over the ~15 year investigation period and averaged over all sites, total relative changes were ~30 and 45% for the (*i*/*n*) ratios of butanes and pentanes, respectively, with a relative increase in the prominence of the *n*-isomers. Most likely causes include changing isomeric ratios in gasoline sector emissions, and increasing influence of oil and natural gas industry emissions. Changes in concentrations and isomeric ratios depend on proximity of contributing emission sources to measurement sites.

1. Introduction

Atmospheric hydrocarbons, excluding methane, are commonly referred to as nonmethane hydrocarbons (NMHCs). NMHCs play a significant role in atmospheric oxidation chemistry. This work investigates atmospheric mixing ratios and (*i*/*n*) isomeric ratios of the NMHCs butane and pentane.

1.1. NMHC Sources

NMHCs have numerous anthropogenic and biogenic sources. Anthropogenic sources are responsible for ~100 Tg NMHC carbon (C) emissions yr^{-1} (World Meteorological Organization, 1995). At 40–45%, alkanes constitute the largest fraction of atmospheric anthropogenic volatile organic compounds (VOCs) in urban environments (Fujita et al., 1992). Despite contributing less than 10% to total global VOC emissions, anthropogenic sources generally dominate air quality in urban areas. The majority of urban alkane emissions are from transportation sector emissions, that is, gasoline and diesel distribution and mobile sources. Atmospheric NMHCs increased from the early 1900s until regulations, such as the Clean Air Act of 1963 and its amendments in 1970, mandated emission reductions from automobiles, oil, and natural gas (O&NG) production, and industrial processes, and led to decreasing trends in urban NMHC mixing ratios (Von Schneidemesser et al., 2010; Warneke et al., 2012). Declining NMHC trends have also been found in records from background monitoring sites and firn air (Aydin et al., 2011; Helmig et al., 2014; Worton et al., 2012). At the peak of atmospheric mixing ratios in the 1970s, automobile emissions were responsible for 75–93% of the NMHC composition in urban air in Los Angeles (LAX) (Mayrsohn & Crabtree, 1976). The *i*-butane and *n*-butane isomers are emitted from a variety of sources, such as biomass burning, petroleum production and use, and natural gas emissions. The *i*-pentane and *n*-pentane isomers have similar sources, but have a relatively larger contribution from liquid fuels (Singh & Zimmerman, 1992). In an urban study, *i*-butane, *i*-pentane, and *n*-pentane were each shown to correlate well with *n*-butane, suggesting that they have similar sources in urban environments (Goldan et al., 1995). In the same study, these alkanes had a weaker correlation with aromatic VOC. Aromatics are predominately a result of vehicle tailpipe emissions; this suggests other significant urban sources of these NMHC alkanes. Later studies showed that butane and pentane isomers were present in petroleum refinery emissions, vehicle running and tailpipe emissions, and gasoline vapor (Pierson et al., 1999; Scheff et al., 1996).

1.2. NMHC Sinks

NMHCs significantly influence tropospheric chemistry, especially the hydroxyl radical, (OH), and ozone (O_3) (Isaksen et al., 1985; Kasting & Singh, 1986; Liu et al., 1987; Trainer et al., 1987). Oxidation by OH is the predominant sink of atmospheric alkanes (Atkinson, 1997). The rate of removal by OH depends on the OH production rate, and as such on atmospheric O_3 and water vapor and the solar flux, and consequently exhibits diurnal and seasonal cycles (Jobson, Niki, et al., 1994; Rudolph & Ehhalt, 1981). NMHCs are also oxidized by nitrate (NO_3) and halogen radicals, albeit to a smaller extent (Atkinson, 2000; Penkett et al., 1993). NMHCs are not appreciably photolyzed by wavelengths present in the troposphere. Light alkanes do not react appreciably with O_3, but contribute to tropospheric O_3 production during their atmospheric oxidation (Atkinson & Arey, 2003; Atkinson & Carter, 1984). Neither wet nor dry depositions are significant sinks of light alkanes.

1.3. Use of NMHCs in Atmospheric Research

Atmospheric chemistry research has extensively employed NMHCs. Ratios of NMHC pairs are usually less variable and more consistent than absolute concentrations (Pollmann et al., 2016). They have been used to test the accuracy of tropospheric NMHC measurements, with deviations from expected relationships between compounds indicating sampling and instrument problems (Parrish et al., 1998). NMHC ratios have been used as tracers in emission source and atmospheric oxidation studies. Emission sources have been studied by examining relative compositions of NMHCs (Mayrsohn & Crabtree, 1976). Ratios of NMHCs have been used to estimate rural and urban OH concentrations [OH] (Blake et al., 1993; Calvert, 1976; Roberts et al., 1984). The ratios of acetylene and benzene to NMHC and pentane isomers can be indicators of biomass burning, even after many days of transport (Andreae & Merlet, 2001; de Gouw et al., 2004; Helmig et al., 2008). Lewis et al. (2013) used NMHC to carbon monoxide (CO) ratios to identify biomass burning emissions. Biomass burning, in general, is a larger fractional contributor to atmospheric NMHCs in the southern hemisphere atmosphere, where the largest emission sources are extratropical forest fires and biofuel burning (Andreae & Merlet, 2001; Borner & Wunder, 2012). In many places, biomass burning is the largest contributor to benzene, toluene, ethene, and propene concentrations. Further, *n*-butane and *n*-pentane correlate well with both biomass burning and anthropogenic emissions. Emission factors for NMHCs vary considerably depending on the fuel source and fire type (flaming, smoldering, etc.) (Andreae & Merlet, 2001; Borner & Wunder, 2012).

Halogen chemistry can influence isomeric hydrocarbon ratios, specifically (*i*/*n*) isomer ratios (Gilman et al., 2013; Hornbrook et al., 2016; Jobson, Niki, et al., 1994). While the *i*- and *n*-isomers have similar rate constants for oxidation by OH, increased (*i*/*n*) ratios can indicate chlorine radical chemistry because the *n*-isomers of butane and pentane react faster with chlorine than the *i*-isomers (Swarthout et al., 2013). NMHC ratios, such as the isomeric butane ratio, were used to infer chlorine radical concentrations during the eruption of the Icelandic volcano Eyjafjallajokull (Baker et al., 2011). Gilman et al. (2013) also examined propane/*i*-butane ratios. These compounds have similar chlorine rate coefficients, but *i*-butane has a faster OH rate coefficient than propane. An increase in this ratio indicated an increasing influence of oxidation by OH. Branched alkanes (*i*-isomers) have faster rate constants for reaction with NO_3 than nonbranched alkanes. Rate constants for reaction with NO_3 are 4–5 orders of magnitude lower than with OH. Nonetheless, NO_3 mixing ratios can be high enough to be competitive with OH chemistry, particularly in the winter season at higher latitudes (Atkinson et al., 1986; Penkett et al., 1993; Platt et al., 1980; Wayne et al., 1991).

The dispersion and mixing of emissions from distinct sources are relatively fast compared to butane and pentane photochemical lifetimes, which are on the order of days. Isomeric ratios of these compounds are assumed to be representative of the air mass sampled. Since the OH reaction rate constants of the butane isomers are within 10% (Atkinson & Arey, 2003), relatively consistent (*i*/*n*) isomeric ratios are observed during transport dominated by OH oxidation chemistry from source to downwind regions. Mayrsohn and Crabtree (1976) found an (*i*/*n*) butane isomeric ratio of ~0.5 with σ = 18% despite measuring at four sites with unique conditions in the LAX area. The collection of sites presented by Parrish et al. (1998) showed (*i*/*n*) butane isomeric ratios varying from 0.37 to 0.57. Ratios in this range were found in other studies as well, in both proximity of source regions (Goldstein et al., 1995; Jobson, Wu, et al., 1994) and far downwind (Helmig et al., 2008). Further, there are no notable systematic seasonal changes in the (*i*/*n*) butane isomeric ratio (Helmig et al., 2008).

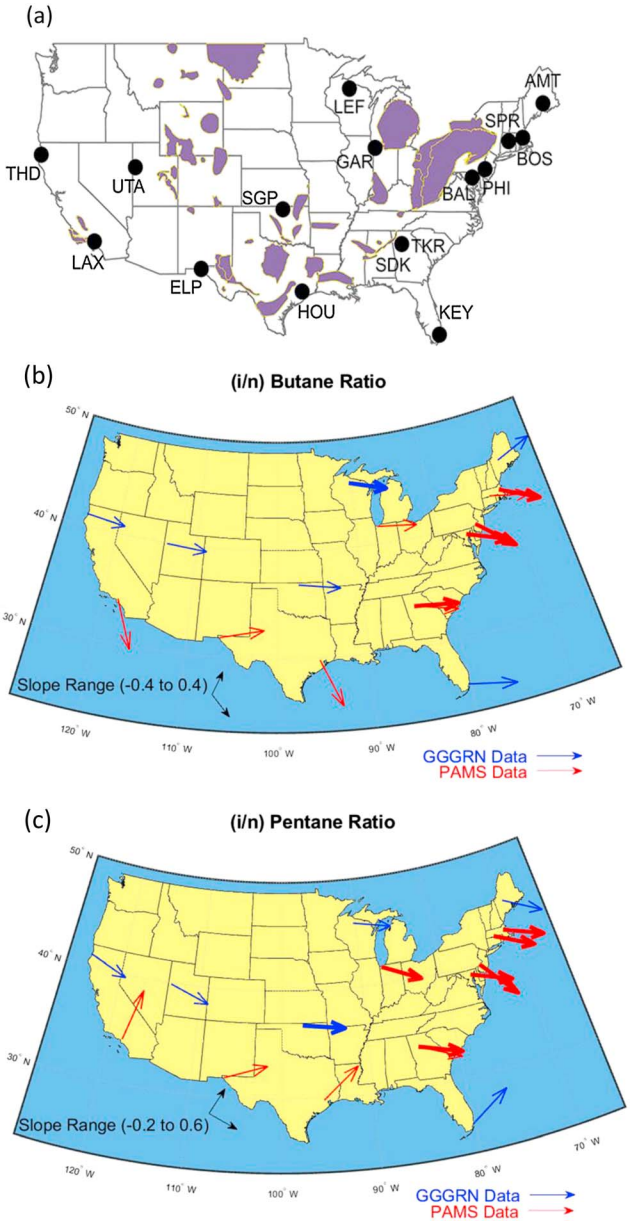

Figure 1. (a) Site locations and their proximity to shale plays. Shale plays are shown in purple; monitoring sites are indicated as black dots. Table 1 lists full site names with the three letter codes used in the map and site coordinates. (b) The (*i*/*n*) butane isomeric ratio trends. (c) The (*i*/*n*) pentane isomeric ratio trends. The solid arrows indicate statistically significant trends; the dotted arrows indicate the rate of change, without this change being a statistically significant trend. Rates of change are in units of yr^{-1}. Photochemical Assessment Monitoring Stations (PAMS) data are in red. Global Greenhouse Gas Reference Network (GGGRN) data are in blue.

A wider range of values is generally observed for the (*i*/*n*) pentane ratio compared to the butane isomeric ratio. Use of the (*i*/*n*) pentane isomeric ratio as an emission tracer was recently demonstrated by Gilman et al. (2013). A ratio of 0.86 indicated O&NG activity, while a ratio of ~2.5 characterized urban emissions. Jobson et al. (2004) found (*i*/*n*) pentane ratios of ~3.3 in HOU at sites influenced by vehicular and industrial emissions. Building on this, Thompson et al. (2014) observed the (*i*/*n*) pentane isomeric ratio in ambient air to determine if increased VOC loading was related to vehicle tailpipe emissions or O&NG development. Helmig et al. (2008) argued that the drop in the (*i*/*n*) pentane isomeric ratio during summer transport events to the Azores, Portugal, was caused by occurrences of biomass burning transport.

Nonisomeric NHMC ratios, such as ln([propane/ethane]) and ln([*n*-butane/ethane]), have been used to study photochemical processing during transport; these ratios have been labeled as "photochemical clocks." Parrish et al. (1992) found that light alkane ratios differed when air masses had different trajectories, and that photochemical aging was consistent with a given trajectory. McKeen and Liu (1993) showed that photochemical aging and transport determine hydrocarbon ratios. Honrath et al. (2008) used these ratios to estimate the age of air parcels transported across the mid-North Atlantic. This work found that it is possible to determine the age of an air parcel making assumptions about source region hydrocarbon emission ratios and mean [OH]. The ln([propane/ethane]) ratio has also been used to investigate O_3 production as a function of transport and the seasonal photochemical processing (Helmig et al., 2008, 2015; Honrath et al., 2008).

In summary, a myriad of atmospheric research has focused on light NMHCs and their ratios. Much of this research relies on the assumption of temporarily and regionally consistent NMHC ratios in source regions. This condition is preemptive to identify sampling inconsistencies, studies on the aging of an air mass, and emission sources as discussed above. Changes in technologies, fuel types, and relative contributions from different emission sources question if and how these isomers and ratios have changed over time. This is evaluated here, utilizing ambient NMHC source region observations from 10 urban monitoring sites in the United States. We also considered data from six mostly background sites for contrasting with the urban data. To our knowledge, the analyses and results presented here are the most comprehensive investigation of isomeric ratios of butanes and pentanes in the continental United States to date.

2. Methods

Considered data are from the U.S. Environmental Protection Agency (EPA) Photochemical Assessment Monitoring Station (PAMS) network and the U.S. National Oceanic and Atmospheric Administration (NOAA) Global Greenhouse Gas Reference Network (GGGRN). Figure 1a shows the site locations; site coordinates are summarized in Table 1.

2.1. PAMS Data

The main objective of PAMS is to maintain an air quality database to evaluate progress toward meeting the O_3 National Ambient Air Quality Standard. PAMS were established in urban areas that were in O_3

Table 1
Site Names, State, Three-Letter Code, Network, Location, Median Isomeric Ratio Over the Full Record and Trend Analysis Results for the (i/n) Butane and (i/n) Pentane Isomeric Ratios

		Coordinates		(*i*/*n*) Butane				(*i*/*n*) Pentane			
	Network	Lat.	Long.	Median	Slope (yr^{-1})	Slope (% yr^{-1})	*P*-value	Median	Slope (yr^{-1})	Slope (% yr^{-1})	*P*-value
Atlanta, GA (SDK)	PAMS	33.8	−84.4	0.68	***−0.003***	***−0.43***	***0.037***	1.9	***−0.043***	***−2.2***	***0.004***
Atlanta, GA (TKR)	PAMS	33.8	−84.4	0.35	−0.006	−1.7	0.45	2.2	−0.060	−2.7	0.26
Baltimore, MD (BAL)	PAMS	39.3	−76.6	0.48	***−0.009***	***−1.9***	***0.021***	1.6	***−0.050***	***−3.1***	***0.003***
Boston, MA (BOS)	PAMS	42.4	−71.1	0.57	***−0.012***	***−2.2***	***0.000***	1.9	***−0.055***	***−2.9***	***0.000***
El Paso, TX (ELP)	PAMS	31.8	−106.4	0.43	0.005	1.1	0.39	2.1	0.042	2.0	0.54
Gary, IN (GAR)	PAMS	41.6	−87.3	0.42	−0.003	−0.59	0.38	1.7	***−0.058***	***−3.3***	***0.000***
Houston, TX (HOU)	PAMS	29.8	−95.4	0.67	***−0.058***	***−8.7***	***0.027***	2.7	0.12	4.5	0.22
Los Angeles, CA (LAX)	PAMS	34.1	−118.3	0.56	−0.056	−10	1.0	2.5	0.55	22	0.46
Philadelphia, PA (PHI)	PAMS	40.0	−75.2	0.57	***−0.021***	***−3.7***	***0.000***	2.5	***−0.17***	***−6.7***	***0.009***
Springfield, MA (SPR)	PAMS	42.1	−72.5	0.60	−0.006	−0.99	0.13	1.8	***−0.069***	***−3.9***	***0.001***
Argyle, ME (AMT)	GGGRN	45.0	−68.7	0.57	0.007	1.2	1.0	1.6	−0.076	−4.7	1.0
Key Biscayne, FL (KEY)	GGGRN	25.7	−80.2	0.50	−0.006	−1.1	0.55	1.3	0.10	7.7	0.23
Park Falls, WI (LEF)	GGGRN	45.9	−90.3	0.45	***−0.006***	***−1.2***	***0.005***	1.3	−0.024	−1.9	0.28
So. Grt. Plns., OK (SGP)	GGGRN	36.6	−97.5	0.40	−0.003	−0.70	0.12	0.98	***−0.015***	***−1.5***	***0.002***
Trinidad Head, CA (THD)	GGGRN	41.1	−124.2	0.56	−0.002	−0.35	0.24	1.5	−0.048	−3.3	0.19
Wendover, UT (UTA)	GGGRN	39.9	−113.7	0.54	−0.002	−0.34	0.53	1.4	−0.050	−3.7	0.27

Note. Statistically significant results are indicated by bold-italic font.

nonattainment in 1997. Sites are classified by their position relative to the urban area and typical morning wind direction. For example, some locations are background sites upwind of the urban area (type 1); others are maximum O_3 concentration sites (type 3), which are about 10 to 30 miles downwind of the urban area. In total, there are 78 PAMS sites. All data in this paper are from type 2 sites, which are maximum O_3 precursor sites. These sites are directly downwind of the urban area's central business district. We chose those sites because we sought the most representative source region data while minimizing the degree of oxidation of these compounds. Data from 10 PAMS sites (Table 1) were used. Sampling occurred between 2000 and 2015, although temporal data coverage varied by site. According to the PAMS protocol, 24 hr integrated samples were collected every sixth day. Samples were collected in canisters and analyzed by gas chromatography with flame ionization detection using a DB-1 column (EPA, 1998) at a series of contracted laboratories. Two calibration standards were used, a propane and benzene mixture as a primary calibration standard, and a standard composed of all target VOC at varying concentrations as a retention time standard. While the same type of sampler is used across the PAMS network, and instruments are calibrated with the same type of standard, site audits have shown that sites averaged an 11.3% deviation error for a variety of compounds against a reference standard analysis (EPA, 1997).

PAMS data were downloaded from the PAMS database (AirNow-DART, https://www.airnowtech.org/dart/dartstatus.cfm, downloaded January 2016) and underwent a filtering routine. First, the median and standard deviation of the data sets were determined for the whole record. Data points three standard deviations above or below the median value were excluded. Next, data were run through a Hampel filter (Davies & Gather, 1993; Pearson et al., 2015). This filter considers a data point and the three points before and after the central point. If the central data point was three standard deviations away from the median of the seven points, it was replaced with the median value. This procedure removed extreme values and improved the data for the purpose of trend analyses because averaged data are considered instead of events. Finally, data were subjected to a running monthly median. An example of a data set before and after applying the filtering routines is shown in Figure S1. Figure S2 shows time series data for all sites after the filtering routine had been performed.

2.2. NOAA/Institute of Arctic and Alpine Research Data

GGGRN Flask data were downloaded from the NOAA Earth System Research Laboratories/Global Monitoring Division database (March 2016) (ftp://aftp.cmdl.noaa.gov/data/trace_gases/voc/). These data are also publicly

available from the World Data Center for Greenhouse Gases (http://ds.data.jma.go.jp/gmd/wdcgg/). There are 46 sites worldwide; data from the six sites in the continental United States were considered here. These samples were collected approximately weekly. NMHC measurements are made by the Atmospheric Research Laboratory at the Institute of Arctic and Alpine Research at the University of Colorado, Boulder, USA, by preconcentrating NMHC onto a microadsorbent trap, followed by thermal desorption and gas chromatography with flame ionization detection (Pollmann et al., 2008). A reference gas calibrated against gravimetrically prepared NMHC standards and containing all butane and pentane isomers was used to calibrate the system weekly. All GGGRN samples have been analyzed on the same instrument, in the same laboratory, and following the same analytical protocol since the beginning of the program (Pollmann et al., 2008), which is advantageous for achieving good comparability between sites. Two audits conducted by the World Calibration Centre for VOC (http://www.imk-ifu.kit.edu/wcc-voc/) yielded analysis result deviations of $<5\%$ for butane and pentane isomers against a series of reference standards. The GGGRN data were first filtered using a NOAA filtering routine (Thoning et al., 1989), and then by the same filtering routine applied to the PAMS data (Figure S1). Filtered data for all sites are available in Figure S2.

2.3. Data Analyses

Isomeric ratio data were determined by dividing the *i*-isomer mixing ratio value by the *n*-isomer value in a given sample. Samples without a matching measurement result for the other isomer were excluded. Filtering removed outliers and reduced the range of data. This yielded a more reliable representation of the behavior of the whole data set. Once filtered, a variety of analyses were conducted:

Seasonal Cycles - Data at each site were sorted by collection month. A box-whisker plot was constructed for each month's data to investigate the average seasonal cycle. In all box plots, the center red line is the median of the data considered for the box, the top of the box indicates the data's upper 75^{th} percentile, the bottom of the box the lower 25^{th} percentile, and whiskers correspond to $\pm$ 2.7 times the standard deviation of the data.. Relative seasonal amplitudes were calculated by subtracting the lowest monthly median from the highest monthly median and dividing by each site's overall median mixing ratio.

Multi-Year Changes - The box-whisker plots for each year of data were plotted against the observation year. Relative yearly ranges were determined by calculating the median mixing ratio for each calendar year, and subtracting the lowest annual median from the highest annual median, and then dividing by the site's overall median across all years of available data. This quantifies the variability observed over each site's available data.

2.4. Trend Analyses

Statistical trend analyses were conducted by calculating the median for each calendar year at each site and subjecting the time series of medians to a Mann-Kendall test (Hirsch et al., 1991; Kendall, 1975; Mann, 1945) to determine the presence of a trend over the entirety of the record. Trends were tested at the 95% confidence level. Trend values were calculated using a Theil-Sen robust linear regression (Sen, 1968; Theil, 1950). The Theil-Sen method is a nonparametric technique for quantifying a linear trend because it is resistant to outliers. Relative trends for each site were found by dividing the Theil-Sen slope result by each site's overall median mixing ratio. A *p*-value less than 0.05 indicates a statistically significant trend at 95% confidence. Some of the sites, that is, LAX, Argyle, and Key Biscayne (KEY), had less than a 10 year record. These shorter records yield a reduced statistical power (Hatch, 2003), which could result in an acceptance of the null hypothesis despite the absence of a trend. For more discussion on statistical power, please refer to Text STx1.

3. Results

Time series plots for all four isomers at all sites are available in Figures S2a–S2o. The tables below summarize the mean mole fraction and trend analysis results. Table 1 lists *p*-values, trend slopes, slope percentiles, and trend significance results for each of the (*i*/*n*) butane and pentane isomer ratios. Table 2 shows these results for each of the individual butane and pentane isomers. Tables 3 and 4 show relative seasonal amplitudes and relative yearly ranges of mixing ratios for each isomer and ratio.

Table 2
i-Butane, n-Butane, i-Pentane, and n-Pentane Median Mixing Ratios, Trend Slopes, and P-Values

	i-Butane				*n*-Butane			
	Median (nmol mol^{-1})	Slope (nmol mol^{-1} yr^{-1})	Slope (% yr^{-1})	*P*-value	Median (nmol mol^{-1})	Slope (nmol mol^{-1} yr^{-1})	Slope (% yr^{-1})	*P*-value
Atlanta (SDK)	2.75	***−0.150***	***−5.45***	***0.000***	4.00	***−0.200***	***−5.00***	***0.001***
Atlanta (TKR)	1.90	−0.070	−3.68	0.573	5.40	−0.320	−5.93	0.060
Baltimore	1.80	***−0.086***	***−4.76***	***0.004***	3.61	−0.113	−3.14	0.080
Boston	1.15	***−0.050***	***−4.35***	***0.049***	1.80	−0.054	−2.98	0.063
El Paso	3.56	−0.197	−5.52	0.174	6.72	−0.128	−1.90	0.266
Gary	1.40	−0.040	−2.86	0.208	3.34	−0.049	−1.47	0.208
Houston	11.7	***−1.80***	***−15.4***	***0.027***	16.8	−2.26	−13.5	0.220
Los Angeles	2.99	−0.025	−0.84	1.000	4.72	0.085	1.80	0.806
Philadelphia	3.80	***−0.349***	***−9.20***	***0.002***	5.93	***−0.426***	***−7.18***	***0.009***
Springfield	1.20	−0.026	−2.20	0.217	1.85	−0.015	−0.84	0.337
Argyle	0.083	−0.012	−14.0	1.000	0.139	−0.016	−11.6	1.000
Key Biscayne	0.033	−0.002	−5.38	0.230	0.061	−0.000	−0.70	0.548
Park Falls	0.078	***−0.004***	***−5.52***	***0.029***	0.168	−0.007	−3.86	0.161
So. Grt. Plains	0.407	***0.032***	***7.75***	***0.005***	1.02	***0.095***	***9.39***	***0.000***
Trinidad Head	0.044	0.001	2.22	0.304	0.070	0.003	4.33	0.086
Wendover	0.041	−0.002	−5.90	0.062	0.069	***−0.003***	***−4.61***	***0.029***

Note. Statistically significant results are indicated by bold-italic font.

3.1. Absolute Mole Fractions

We chose Trinidad Head (THD) as a reference to compare and contrast with the urban PAMS data. THD is located on the Northern California Pacific coast, largely free from nearby anthropogenic influence. With prevailing winds coming from the Pacific Ocean, most air sampled at THD reflects the marine Pacific background atmosphere. The upper panel of Figure 2 shows seasonal cycles and isomeric ratios at THD. For comparison, seasonal cycles for the same compounds and isomer ratios for the inner city PAMS Atlanta-SDK (SDK) site are shown in the lower panel. Please note the different mole fraction scales (*y*-axis) of the two sets of plots, indicating the on average ~100 times higher butane and pentane mole fractions in the Atlanta urban atmosphere compared to THD. Of the considered PAMS sites, SDK falls into about the middle range of observed butane and pentane mixing ratios (Table 2), making it a representative example for illustrating the influence of urban anthropogenic emissions. The corresponding plots for all other sites are presented in Figures S3a–S3p.

Mixing ratios of individual isomers at PAMS sites were highest for *i*-pentane, followed by *n*-butane, *n*-pentane, and *i*-butane. At GGGRN sites, mixing ratios were highest for *n*-butane followed by *i*-butane, *i*-pentane, and *n*-pentane. This was determined by finding the median of all sites' mixing ratios for each isomer. Median mixing ratios at PAMS sites were 2–3 orders of magnitude larger than GGGRN sites, with the exception of SGP, which had mixing ratios ~10 times higher than other GGGRN sites for all isomers. The highest mixing ratios for all isomers were observed at the HOU site, ranging from 6.13 to 16.8 nmol mol^{-1}. The lowest mixing ratios for three of the four isomers were observed at KEY, and ranged from 0.030 to 0.061 nmol mol^{-1}. THD displayed lowest mixing ratios for *n*-pentane (0.022 nmol mol^{-1}). Median mixing ratios for all isomers at all sites are available in Table 2.

Butane (*i*/*n*) ratio values ranged from 0.352 at Atlanta-TKR (TKR) to 0.677 at SDK. Pentane (*i*/*n*) ratio values ranged from 0.980 at SGP to 2.70 at HOU. Butane ratios were similar at PAMS and GGGRN sites, but pentane ratios were, on average, higher at PAMS sites than at GGGRN sites. Median butane and pentane isomeric ratios observed at all sites are available in Table 1.

3.2. Yearly Ranges

The year-to-year differences in median mixing ratios, here termed "yearly ranges," were studied to determine the interannual variability. Yearly ranges can identify changes in emission profiles that do not necessarily result in a consistent trend from year to year. Yearly range data for butanes and pentanes for selected sites are summarized in Tables 3 and 4, and yearly range plots in Figures S4a–S4p, respectively. The largest yearly ranges for

Table 2 *(continued)*

	i-Pentane				*n*-Pentane			
	Median (nmol mol^{-1})	Slope (nmol mol^{-1} yr^{-1})	Slope (% yr^{-1})	*P*-value	Median (nmol mol^{-1})	Slope (nmol mol^{-1} yr^{-1})	Slope (% yr^{-1})	*P*-value
Atlanta (SDK)	4.35	***−0.239***	***−5.49***	***0.003***	2.40	***−0.150***	***−6.25***	***0.002***
Atlanta (TKR)	6.70	0.000	0.00	1.000	2.90	0.100	3.45	0.452
Baltimore	4.52	*−0.251*	*−5.55*	0.006	2.54	−0.030	−1.18	0.250
Boston	2.00	***−0.167***	***−8.33***	***0.002***	1.05	***−0.029***	***−2.80***	***0.001***
El Paso	8.45	***−0.946***	***−11.2***	***0.009***	3.90	***−0.431***	***−11.1***	***0.026***
Gary	2.73	***−0.167***	***−6.12***	***0.012***	1.50	−0.038	−2.56	0.125
Houston	16.4	1.6	9.76	0.806	6.13	−0.625	−10.2	0.462
Los Angeles	9.51	2.22	23.4	0.296	3.53	−0.080	−2.27	1.000
Philadelphia	10.8	***−1.03***	***−9.55***	***0.014***	3.90	***−0.142***	***−3.63***	***0.019***
Springfield	2.10	***−0.092***	***−4.39***	***0.034***	1.10	0.000	0.00	1.000
Argyle	0.102	−0.025	−24.3	1.000	0.064	−0.006	−9.92	1.000
Key Biscayne	0.030	−0.001	−2.20	0.368	0.024	−0.002	−9.07	0.133
Park Falls	0.078	***−0.003***	***−4.30***	***0.005***	0.056	−0.002	−2.69	0.161
So. Grt. Plns.	0.345	0.019	5.54	0.086	0.325	***0.028***	***8.49***	***0.000***
Trinidad Head	0.035	−0.002	−3.38	0.304	0.022	−0.000	−1.52	0.537
Wendover	0.037	*−0.004*	*−11.5*	0.003	0.027	***−0.002***	***−6.00***	***0.029***

i-butane, *n*-butane, and *n*-pentane were observed at SGP; the largest *i*-pentane yearly range was at Gary (GAR). TKR exhibited the smallest yearly ranges for the butane isomers. The smallest yearly ranges for *i*-pentane and *n*-pentane were observed at KEY and Argyle, respectively.

Butane and pentane (*i*/*n*) isomeric ratio yearly ranges were generally smaller than for individual isomers. The lowest butane ratio yearly ranges were observed at SDK and SGP; the largest was in HOU. The lowest pentane ratio yearly range was observed at TKR, and the largest value was in LAX. Yearly ranges of these ratios for all sites are in Tables 3 and 4.

3.3. Seasonal Amplitudes

Seasonal amplitude data from THD, as seen in the upper panel of Figure 2, show a good example of how the butane and pentane isomers behave in the background atmosphere. Note that mixing ratios are less variable within a given month at THD than at SDK, and 1 to 2 orders of magnitude lower. Seasonal amplitude plots for butanes and pentanes at all other sites are available in Figures S3a–S3p. Seasonal cycles for the individual isomers at the PAMS SDK site are not as pronounced as at THD (Figure 2). The smaller relative seasonal amplitudes at SDK show the stronger influence of local emissions. A comparison of the relative amplitudes of the seasonal cycle as a function of median mixing ratios and the relative seasonal cycle of isomeric ratios as a function of the median isomeric ratio, illustrated in Figure 3, shows that relative seasonal amplitudes are lower, and median mixing ratios are higher for the individual isomers at PAMS sites in comparison to GGGRN sites, but there are no clear trends within the site types. These results show that near the sources (PAMS sites), ambient levels are more dependent on emissions than on photochemical processing (GGGRN sites). All seasonal amplitudes were positive for *i*-butane and *n*-butane, indicating that mixing ratios were always higher in winter than summer. Negative seasonal amplitudes were observed at three and four sites for *i*-pentane and *n*-pentane; all of these sites were PAMS sites. The most negative amplitudes for both isomers were observed in Boston (BOS). The largest seasonal amplitudes were observed at THD for three of the four isomers; the largest seasonal amplitude for *i*-butane was at KEY. The smallest seasonal amplitudes for *i*-butane and *n*-butane were in HOU. Seasonal amplitudes for all isomers at all sites are in Tables 3 and 4.

All (*i*/*n*) butane ratio seasonal amplitudes at PAMS sites were negative. Seven of 10 (*i*/*n*) pentane ratio seasonal amplitudes at PAMS sites were negative. Half of the amplitudes of both butane and pentane isomer ratios were negative at GGGRN sites. Seasonal amplitudes of the butane ratio ranged from −0.41 at HOU to 0.32 at Park Falls (LEF). Seasonal amplitudes of the pentane ratio ranged from −0.29 at BOS and THD to 0.78 at Philadelphia (PHI). All butane and pentane ratio seasonal amplitudes are available in Tables 3 and 4.

Table 3
Relative Seasonal Amplitudes and Relative Yearly Ranges of Butane Isomers and (i/n) Butane Isomeric Ratio at All Sites

	i-Butane		*n*-Butane		Butane isomeric ratio	
Site	Seasonal amp.	Yearly range	Seasonal amp.	Yearly range	Seasonal amp.	Yearly range
Atlanta (SDK)	0.89	0.87	1.00	0.75	−0.11	0.10
Atlanta (TKR)	0.74	0.32	0.94	0.37	−0.24	0.19
Baltimore	0.74	0.79	1.11	0.68	−0.27	0.45
Boston	0.70	0.93	0.97	0.74	−0.16	0.34
El Paso	1.06	2.45	1.29	0.89	−0.26	0.37
Gary	0.80	1.36	1.08	1.71	−0.31	0.47
Houston	0.12	0.98	0.60	1.35	−0.41	1.11
Los Angeles	0.70	0.61	1.41	0.48	−0.33	0.48
Philadelphia	0.91	1.32	0.99	1.10	−0.24	0.74
Springfield	1.08	1.54	1.27	0.89	−0.15	0.42
Argyle	1.87	0.46	1.98	1.62	−0.08	0.28
Key Biscayne	1.24	0.63	1.32	0.63	−0.26	0.53
Park Falls	2.10	0.69	1.70	0.62	0.32	0.14
So. Grt. Plains	0.85	2.46	0.89	2.38	0.06	0.10
Trinidad Head	2.04	1.28	2.33	1.38	−0.13	0.22
Wendover	1.42	1.12	1.68	1.50	0.10	0.32

3.4. Changes Over Time in Absolute Levels and Isomeric Ratios

Theil-Sen linear regression of annual median data was used to investigate changes over time in absolute values and isomeric ratios, with regression slope values used as indicators of the rate of change. These analyses yielded some similarities between sites, although no two sites were identical with respect to statistically significant trends. Tables 1 and 2 summarize results for all sites and compounds; italicized results indicate statistically significant trends. Table STb1 shows the confidence intervals for the trend slopes shown in Tables 1 and 2. Figures 4a and 4b display results graphically for sites with statistically significant (*i*/*n*) alkane isomeric ratio trends along with THD. Results for other sites are shown in Figures S4a–S4p. Figure 5 presents a summary of slope results for all isomers and (*i*/*n*) isomeric ratios at all sites, with squares representing statistically significant trend slopes.

Mixing ratios of the butane and pentane isomers have been decreasing at most of the sites, that is, 81% considered in this study. The magnitude of these changes varies widely across the United States, i.e., −15 to 7.8% year^{-1} for *i*-butane, −14 to 9.4% year^{-1} for *n*-butane, −24 to 23% year^{-1} for *i*-pentane, and −11 to

Table 4
Relative Seasonal Amplitudes and Relative Yearly Ranges of Pentane Isomers and (i/n) Pentane Isomeric Ratio at All Sites

	i-Pentane		*n*-Pentane		Pentane isomeric ratio	
Site	Seasonal amp.	Yearly range	Seasonal amp.	Yearly range	Seasonal amp.	Yearly range
Atlanta (SDK)	0.43	0.90	−0.08	1.04	0.51	0.44
Atlanta (TKR)	−0.05	0.57	0.00	0.67	−0.10	0.15
Baltimore	0.09	1.37	0.19	0.47	−0.17	0.59
Boston	−0.38	1.51	−0.10	1.10	−0.29	0.42
El Paso	0.40	0.94	0.65	1.53	−0.20	0.38
Gary	0.17	2.13	0.47	1.80	−0.19	0.55
Houston	−0.14	0.71	−0.01	1.14	−0.13	0.48
Los Angeles	0.89	1.50	0.32	0.62	0.15	2.04
Philadelphia	0.66	1.58	−0.02	1.32	0.78	1.20
Springfield	0.14	1.02	0.45	0.86	−0.19	0.44
Argyle	0.96	0.49	0.85	0.43	−0.17	0.29
Key Biscayne	0.60	0.40	0.70	1.13	0.12	1.02
Park Falls	1.23	0.69	1.28	0.62	−0.23	0.42
So. Grt. Plains	0.93	1.63	0.73	1.99	0.04	0.29
Trinidad Head	1.47	0.78	1.63	0.82	−0.29	0.61
Wendover	0.83	1.56	0.69	1.02	0.11	0.65

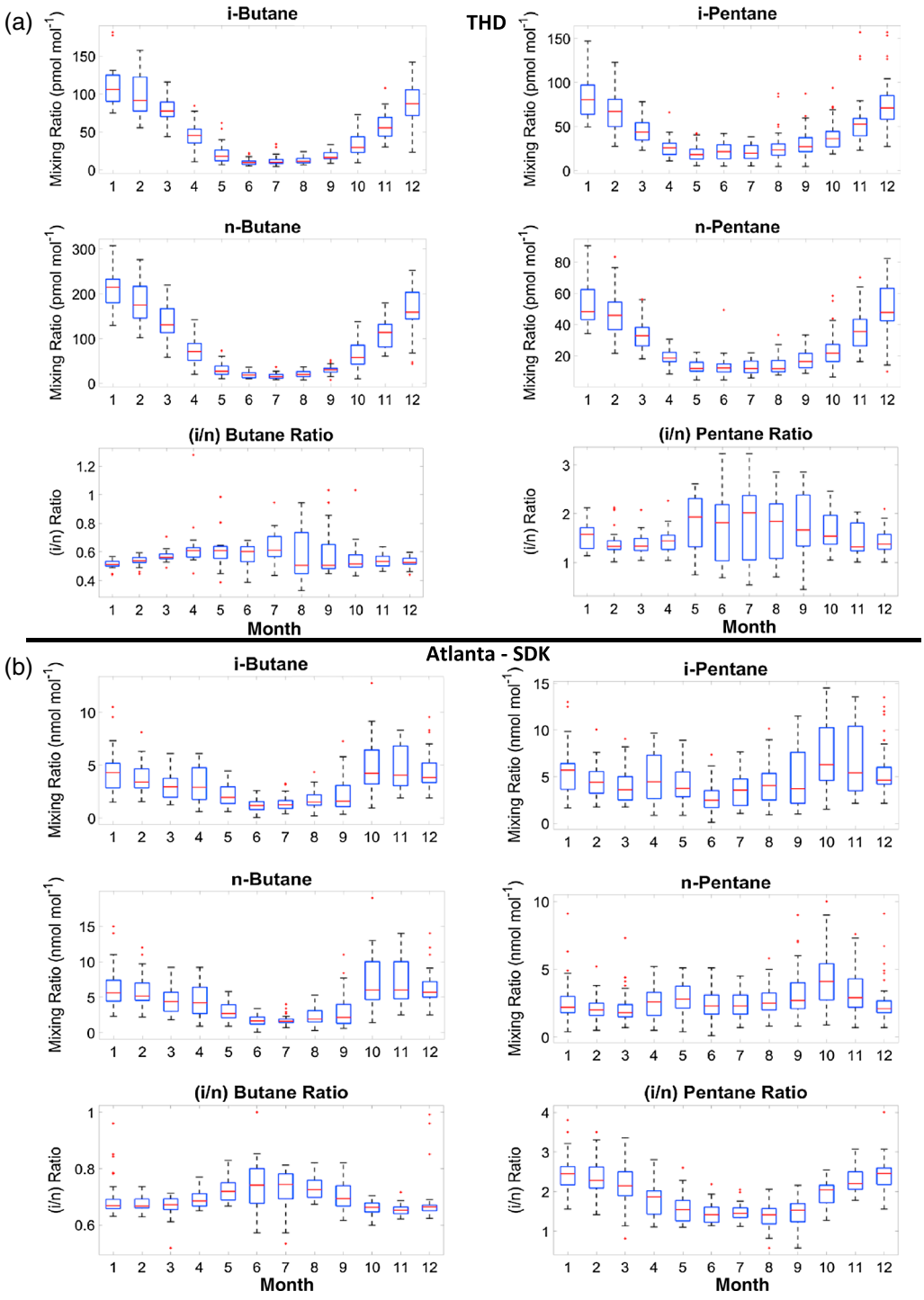

Figure 2. Statistical analysis results of monthly butane and pentane isomers and (*i*/*n*) isomeric ratio data at THD (a) and Atlanta-SDK (b). Note that different scales and units are used for the *y* axis in both the top and bottom panels.

8.5% year^{-1} for *n*-pentane. Similarly, large ranges were observed in changes of the (*i*/*n*) butane and pentane isomeric ratio (−10 to 1.2% yr^{-1}, and −6.7 to 22% yr^{-1}, respectively). SGP was the only site where statistically significant positive trends were observed (for *i*-butane, *n*-butane, *n*-pentane). The most negative, statistically significant trends were observed at PHI for all isomers, except for *n*-pentane; El Paso's *n*-pentane rate of change was the most negative. The only PAMS site with positive rates of change for any isomer was LAX, with positive slopes for *n*-butane and *i*-pentane, which is not consistent with Warneke et al. (2012). However, the

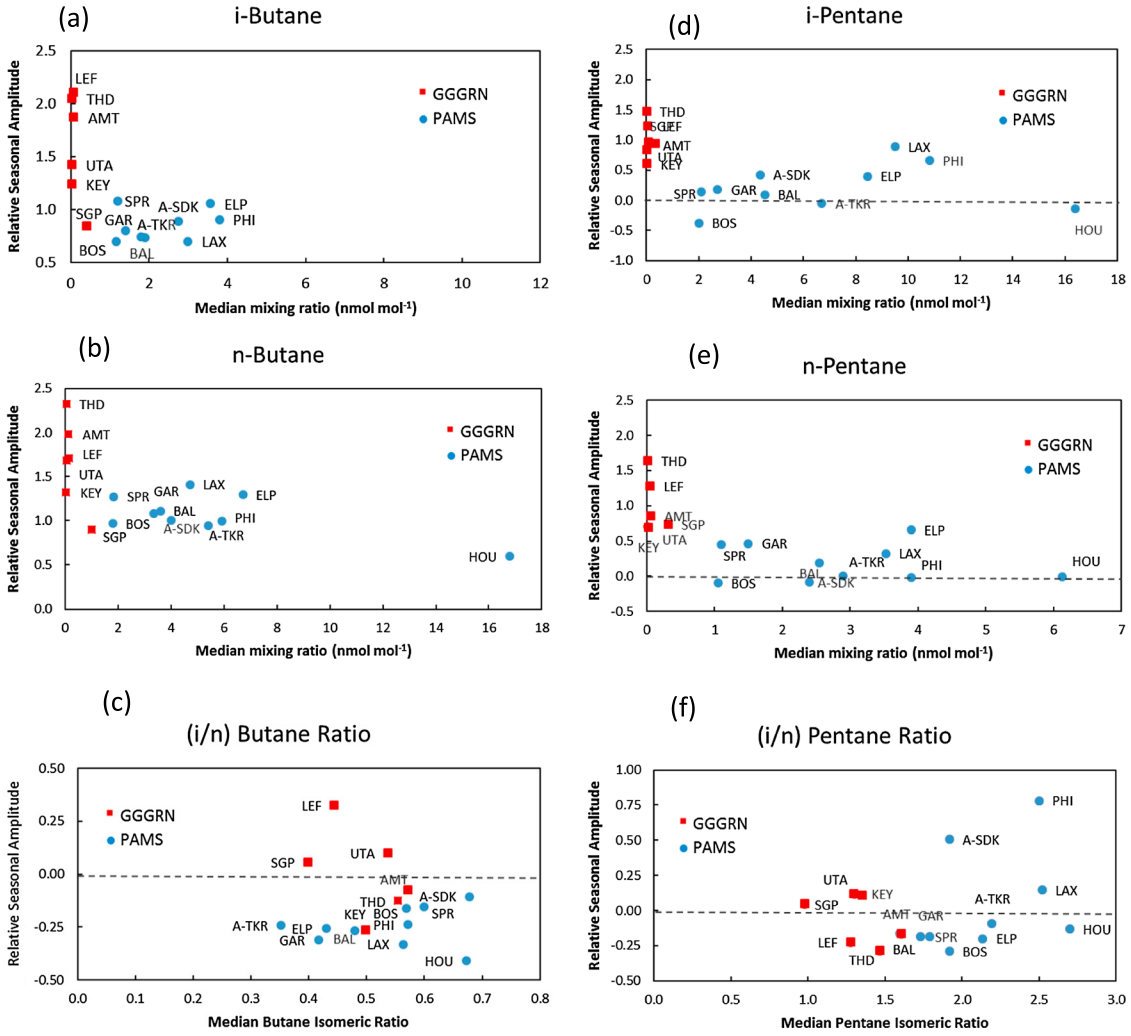

Figure 3. Seasonal amplitudes of butane isomers, pentane isomer, and their isomeric ratio as a function of the annual median mixing ratios. Global Greenhouse Gas Reference Network (GGGRN) sites data are in red; Photochemical Assessment Monitoring Stations (PAMS) data are in blue. Axis ranges vary by plot.

slopes for LAX were far from statistically significant (p-value = 0.806 and 0.296, for n-butane and i-pentane) and are positive as a result of higher medians observed in 2014 and 2015; these years were not included in the Warneke et al. (2012) analyses. Further, the LAX PAMS record included only five years of data, giving the 2014 and 2015 data a high influence over the slope result.

All statistically significant trends for the isomer ratios were negative. Six sites had statistically significant negative trends for the (i/n) butane isomeric ratio. Four of these are East Coast cities (Atlanta, Baltimore (BAL), BOS, and PHI). The most negative was at HOU. The pentane isomeric ratio had statistically significant negative trends at seven sites (Figure 4b), with six of these sites located east of the Mississippi River (SDK, BAL, BOS, GAR, PHI, and Springfield [SPR]).

4. Discussion

4.1. Changes in Isomer Absolute Mole Fractions

Results for individual compounds and sites vary rather widely. It is likely that a fraction of the observed spread and variability in results from different sites, in particular from the PAMS network, may arise from a relatively lower measurement precision (larger measurement uncertainty), as different instruments and laboratories were used for the measurements (see section 2). A common feature in the data are the mostly declining atmospheric mole fractions across sites within both networks. Average (PAMS + GGGRN) atmospheric

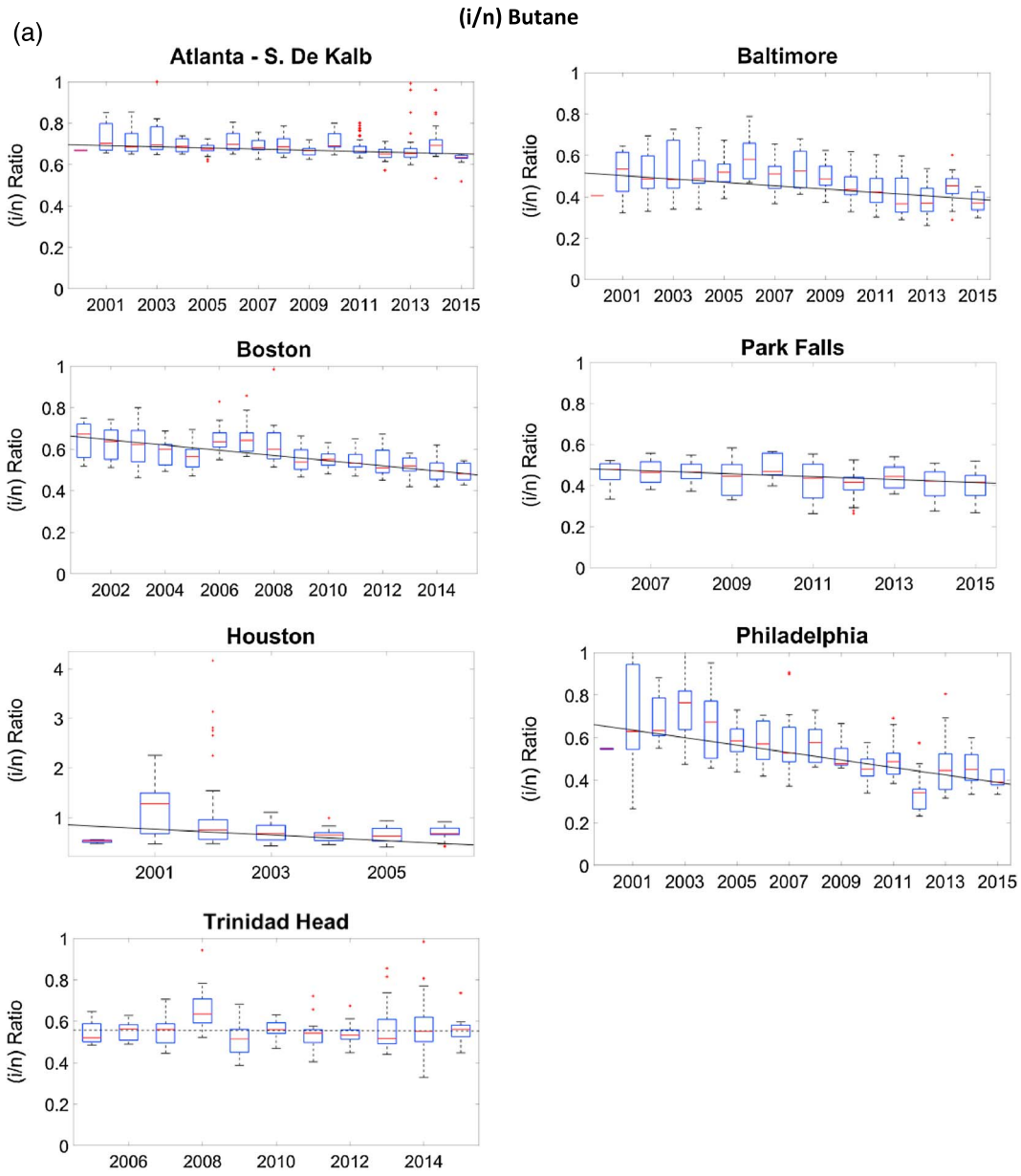

Figure 4. (a). Sites with statistically significant (*i/n*) butane isomeric ratio trends. (b) Sites with statistically significant (*i/n*) pentane isomeric ratio trends. The solid trend line indicates a statistically significant trend; a dotted line indicates no trend is present. Medians without boxes are shown for years with incomplete data coverage. Trinidad Head does not display a trend and is included as background reference site.

mole fraction declines for the 2000–2015 time window were (overall median of slope values among sites with 1-σ standard deviation) −5.1 ± 5.3, −3.1 ± 5.4, −4.9 ± 10.1, and −2.7 ± 5.0% yr^{-1} for *i*-butane, *n*-butane and *i*-pentane, *n*-pentane, respectively. This finding is in agreement with other previous work that has shown declining light NMHCs in U.S. urban atmospheres (Bishop & Stedman, 2008; Warneke et al., 2012). This general behavior is also in accord with observations outside of the United States, mainly in Europe, where urban NMHCs have been steadily declining since ~1990 (Derwent et al., 2017; Monks et al., 2009; Von Schneidemesser et al., 2010). As mentioned earlier, a recent study of C2–C8 hydrocarbons in the United Kingdom using 1993 to 2012 data found declining concentrations of most ≥C4 VOC, whereas ethane and propane concentrations have remained near 1993 values (Derwent et al., 2017).

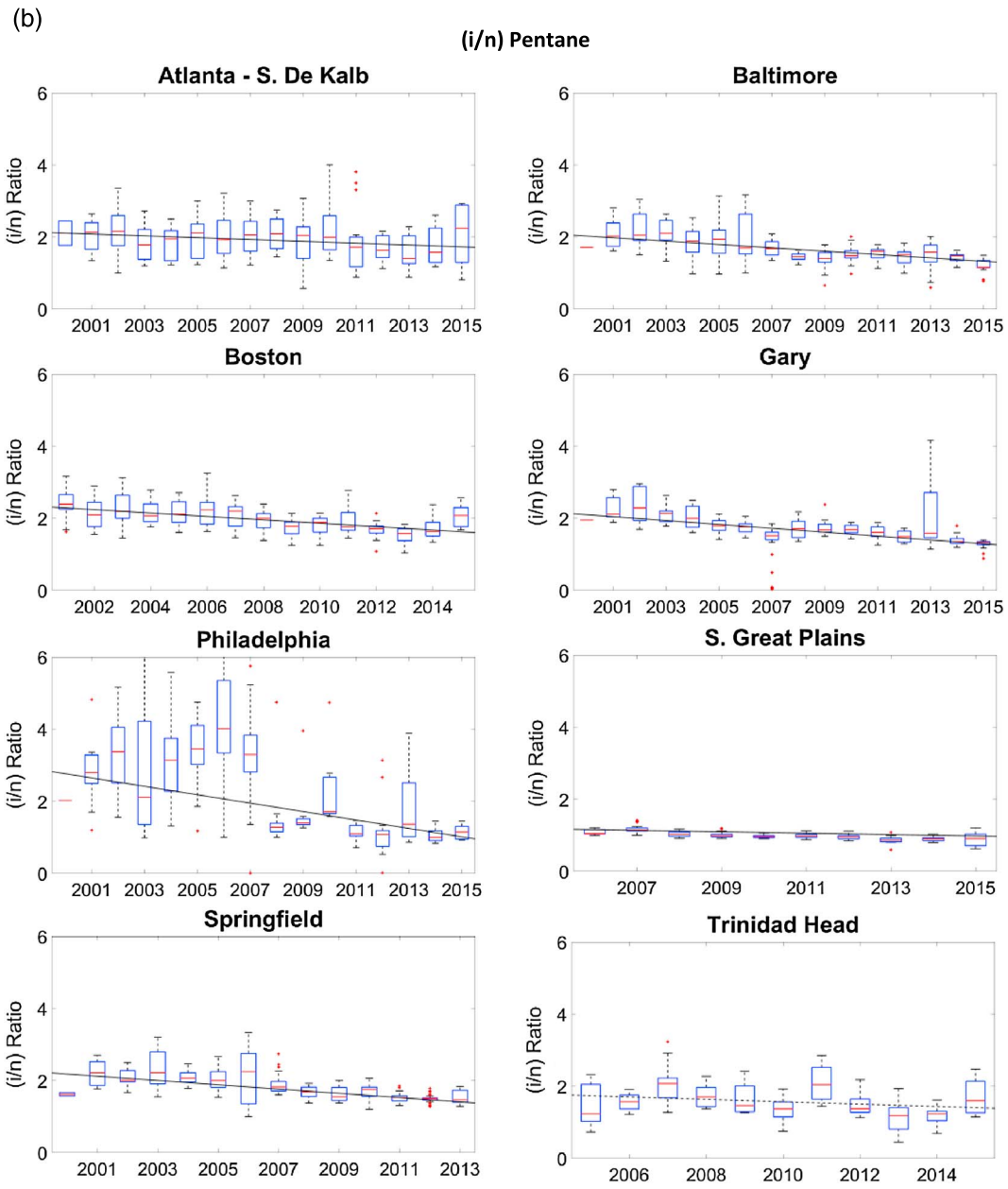

Figure 4. (continued)

4.2. Factors Influencing Observed Seasonal Amplitudes

The observed seasonal amplitudes in the data are expected to be the net effect of chemistry, boundary layer dynamics, and emissions. With reaction by OH being the primary removal of these NMHCs, lower mixing ratios are naturally expected during the summer, when the removal rate is higher due to the higher summertime [OH]. Diurnal and seasonal boundary layer height (BLH) dynamics are another variable exerting an influence on the NMHC seasonality at the surface. BLH determines the rate of dilution of surface-based emissions, and depends on multiple variables, including surface type, topography, and vegetation land cover (Stull, 1988). Daytime maxima BLH can be as high as 5 km over low-latitude deserts and as low as 0.5 km over the ocean (Garratt, 1992). Further, BLH varies by season, typically being higher in summer (Seidel et al., 2012). Coastal sites, such as THD, have on average lower BLH and less seasonal variation of BLH than inland sites. This would be expected to result in a weaker dilution of surface emissions, and a lower seasonal influence by BLH dynamics exerted on seasonal NMHC cycles. However, the amplitude of the seasonal cycle at THD is among

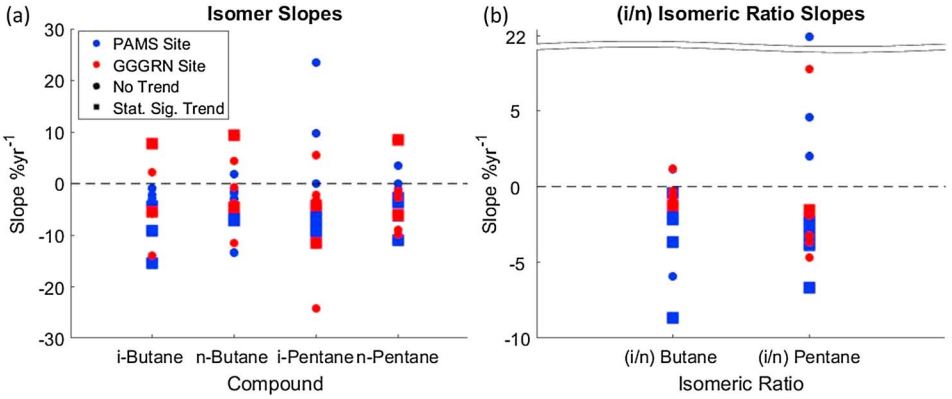

Figure 5. Summary plots of (a) butane and pentane isomers and (b) (*i*/*n*) isomeric ratio trend analysis and linear regression slopes observed at all sites. Photochemical Assessment Monitoring Stations (PAMS) sites are in red, Global Greenhouse Gas Reference Network (GGGRN) sites are in blue. The square points indicate a statistically significant trend at 95% confidence. Circular points indicate rate of change results, without the value being a statistically significant trend. The legend in (a) applies to (b) as well.

the largest relative seasonal amplitudes observed in this work. This large signal is likely predominantly driven by the seasonal cycle of oxidation chemistry. From the BLH consideration, larger seasonal amplitude signals would be expected at the inland sites from stronger dilution during the summer (deeper BLH). This generally is not observed in the data: The urban sites on average display the smallest relative seasonal amplitude. This behavior can be taken as an indication that proximity to and strength of emissions exert an overall stronger influence than the seasonal BLH and oxidation chemistry cycles at these locations.

The (*i*/*n*) butane isomeric ratio displayed a seasonal cycle, peaking in the summer at all sites as indicated by negative values in Figure 3c except LEF, SGP, and UTA (Figure 2 for THD and SDK, Figure S3 for all other sites). The (*i*/*n*) pentane isomeric ratio peaked in the summer at seven PAMS sites and three GGGRN sites (Figure 3f). The summer peak in this ratio is expected from chemical considerations. The *n*-isomers have the slightly faster OH reaction rate constants of the isomeric pairs, resulting in a relatively faster removal of the *n*-isomer at the higher summertime [OH] and higher (*i*/*n*) isomeric ratios. Further, the relative differences of the reaction rate constants of these isomers with OH increase during the summer from their OH reaction rate temperature dependences (Figure S6) (Atkinson, 2003; Wilson et al., 2006). If emissions were constant, one could expect an ~5% and 7% seasonal variation of isomeric ratios of butanes and pentanes, respectively, from the reaction rate constant temperature dependency alone (Figure S6). Combined, these two effects result in an overall relatively faster removal rate of the *n*-isomer and higher (*i*/*n*) isomeric ratios in the summer.

4.3. Isomeric Ratios and Trends

Over the 15 year study period declining (*i*/*n*) isomeric ratio trends were observed at the majority of sites. The median rates of change (overall (all sites) median of determined slope values with 1-σ standard deviation) were $-1.0 \pm 3.1\%\ yr^{-1}$ for the (*i*/*n*) butane and $-2.8 \pm 6.9\%\ yr^{-1}$ for the (*i*/*n*) isomeric pentane ratio. If only statistical significant cases are considered, then median results are $-2.0 \pm 3.0\%\ yr^{-1}$ for the (*i*/*n*) butane, and $-3.1 \pm 1.6\%\ yr^{-1}$ for the (*i*/*n*) isomeric pentane ratio. Over the ~15 year investigation period these values account to total changes of ~30 and 45% for these isomeric ratios.

Previously published (*i*/*n*) butane isomeric ratios ranged from ~0.4 to 0.6 (Goldstein et al., 1995; Jobson, Niki, et al., 1994; Parrish et al., 1998). The median (*i*/*n*) butane isomeric ratios observed in the data considered in this study (0.35–0.68) mostly fall within this range. The center of the distribution is similar, but the results across PAMS and GGGRN sites suggest a larger range of values than previous work that mostly focused on individual site observations.

The relative ratio of isomeric pentane emissions varies widely among emission categories and study region (Andreae & Merlet, 2001; Gilman et al., 2013; Helmig, Thompson, et al., 2014; Jobson et al., 2004; LaFranchi et al., 2013; Peischl et al., 2013; Pétron et al., 2012; Swarthout et al., 2013, 2015) (Table STb2). The observed changes seen in the data considered here could be due to changes in sources, sinks, or a combination of

both. Likely, the relative influence of these processes will vary between urban, semiurban, semirural, and rural locations. In the following we will discuss a series of probable causes.

4.4. The Influence of Mobile Sources on Isomers and Ratio Trends

Since transportation sector/mobile source-related emissions are a major source of atmospheric butane and pentane isomers, it is likely that these results reflect a series of obvious changes in gasoline composition, consumption, tailpipe emissions, and evaporative losses. In 2004, at least 45 different blends of gasoline were produced in the United States. This myriad of blends developed because as of 2005, the U.S. EPA could not deny a special blend of gasoline compliant with the Clean Air Act (1963) and its amendments (1970) (Wells, 2005). VOC emission reduction is primarily achieved by lowering a fuel's Reid Vapor Pressure (EIA, 1998). There has been a notable reduction of the VOC fraction in gasoline formulations used in U.S. cities. In California, a reformulated gasoline blend was estimated to have a 25–29% lower fraction of VOCs compared to conventional gasoline used before 1995. Similarly, during 1995–2006, volatiles in gasoline declined by 26.6–30.2% in BOS, Chicago, GAR, PHI, BAL, SPR, and HOU (EPA, 2006a, 2006b, 2006c, 2006d, 2006e, 2006f) in comparison to conventional formulations of gasoline used before 1995. Tailpipe emissions of hydrocarbons from light-duty gasoline vehicles were reduced by a factor of 100 from 1968 to 2004 (Faiz et al., 1996) from technical improvements, such as catalytic converters, evaporative emissions control systems, computer controlled fuel injection, and engine efficiency (McDonald et al., 2013). These VOC reformulations and emission reductions from the transportation sector are likely explanations for the decreasing mixing ratios of butane and pentane isomers in urban areas. Obviously, these reductions have superseded expected emission increases from the steady growth of the automobile fleet across the nation.

Changes in gasoline formulations could also play a role in seasonal changes in butane and pentane isomers and their ratios. Special blends of gasoline are often developed in response to air quality standards in a particular region or time of year (EPA, 2017). Winter formulations of gasoline can include higher concentrations of butane and pentane isomers without violating regulations (Wells, 2005). The *n*-butane isomer is present in higher concentrations in wintertime gasoline (Goldstein et al., 1995) because of its high octane rating (94), but its high vapor pressure prevents it from being used in high concentrations in summertime gasoline.

4.5. Possible Influence of O&NG Development on Isomers and Ratios

The volume of the shale gas production in the United States increased by a factor of 4 from 2009 to 2014 (EIA, 2017). O&NG development is a common source of atmospheric alkanes, and recent studies have shown increasing influence and dominance of O&NG emissions on observed atmospheric NMHCs within and downwind of O&NG basins (Gilman et al., 2013; Helmig et al., 2014; Schade & Roest, 2015; Swarthout et al., 2013; Thompson et al., 2014).

SGP provides a case study example for investigating the influence and changes in O&NG emissions on the alkane isomers. SGP is a rural site within the Woodford shale play, which produced some 403 billion cubic feet of shale gas in 2010 (EIA, 2017). There are greater than 60 active oil wells within a 10 mile radius of the SGP monitoring station; a map showing well locations surrounding SGP is shown in Figure S5. The strong influence from O&NG production is apparent in the data shown in Figures 3 and 4b. SGP had highest absolute NMHC levels among GGGRN sites. SGP was also the only site where mixing ratios of all isomers have been increasing. Trends for all isomers were at least 5.5% yr^{-1}, and *n*-butane displayed a slope of 9.4% yr^{-1}. The relative seasonal amplitudes and interannual variability at SGP are the lowest of all sites (PAMS + GGGRN). The (*i*/*n*) pentane isomeric value (dropping from 1.0 in 2006 to 0.9 in 2015) at the end of the record matches the natural gas pentane isomeric ratio in Gilman et al. (2013). As already noted further above, SGP was one of three sites (including LEF and UTA) where the seasonal cycle of the isomeric butane ratio deviated from what would be expected from the seasonality of OH oxidation. A likely explanation is that at these locations the emission influence overwhelms the signal from seasonal OH chemistry seen at the other sites. Collectively, these data features indicate a dominant emission source with constant isomeric ratios, a dominance of emission over photochemical processing, and increasing emissions from nearby O&NG sources.

Across all sites, the pentane isomeric ratio shows a wider range and is a more selective tracer for source attribution than the butane isomeric ratio. While in urban environments an (*i*/*n*) pentane ratio in the range of 2–3 is characteristic, the (*i*/*n*) ratio in O&NG-dominated atmosphere is ~1, as demonstrated for SGP in the preceding paragraph. This difference offers a sensitive tool for deciphering the relative influence of these

two (urban versus O&NG) emission categories on atmospheric NMHCs. Gilman et al. (2013) and Thompson et al. (2014) demonstrated a temporal shift in the isomeric pentane ratio from increasing O&NG emissions. As seen in Figure 4, at the beginning of the time period studied here, every PAMS site that exhibits a statistically significant (*i*/*n*) pentane isomeric ratio trend had an (*i*/*n*) pentane isomeric ratio of at least 2, as typical for an urban environment. By the end of the study period, the (*i*/*n*) pentane ratio had dropped to values below 2 throughout the network, indicating possible increasing influence from O&NG sources at these sites.

Figures 1b and 1c show the trend slope values for the butane and pentane isomeric ratios, and Figure 1a shows the spatial relation of monitoring sites to shale oil and gas plays. There are seven sites directly east of, and within ~200 miles of a shale play that have a statistically significant decreasing (*i*/*n*) pentane isomeric ratio trend: SDK, BAL, BOS, GAR, PHI, SGP, and SPR. With pentane isomeric ratio values of 1.3, LEF gave the second lowest result (after SGP), approaching the signature O&NG isomeric ratio. In a recent survey of ethane and propane trends at ~40 monitoring stations worldwide, LEF had the second highest increasing ethane trend, and fourth highest increasing propane trend among all sites considered (Helmig et al., 2016). Consequently, our results presented here confirm the signature of the previously noted apparent increasing O&NG emissions at LEF, despite major O&NG shales being more than 200 km away from the site (Bakken to the West, and Antrim to the East).

Two of the fastest growing O&NG basins are the Marcellus shale and the New Albany shale. The Marcellus shale has accounted for 85% of U.S. shale production growth since 2012 (Krohn & Nulle, 2015). This shale play is located primarily in Pennsylvania and West Virginia. The data from the sites studied in this work located in Indiana, Maryland, Massachusetts, and Pennsylvania possibly reflect emission changes from the Illinois Basin and the Marcellus Shale. Regional differences in natural gas composition must also be considered in evaluating possible oil and natural gas signatures on observed NMHC. For instance, methane composition of gas produced across Pennsylvania was reported to range from $<$75% methane to $>$90% methane (Burruss & Ryder, 2014; Colon-Roman & Ruppert, 2014). Produced gas from the Marcellus Shale in central and northeast Pennsylvania is considered "dry gas"; it is $>$85% methane with negligible liquid petroleum constituents, making its emissions signature difficult to source using NMHC tracers. Natural gas from Alleghany County in southwestern Pennsylvania, which produced 34 trillion cubic feet of gas from 2000 to 2010 (DEP, 2017), typically has a lower methane composition ("wet gas") and higher concentrations of heavier NMHCs (Demirbas, 2010; Lacey et al., 1934). During west to east air transport, variable emission contributions with different NMHC signatures from both of these O&NG regions would be expected to be sampled at the downwind monitoring locations listed above. All five of the sites in the states mentioned above displayed statistically significant decreasing trends for the (*i*/*n*) pentane isomeric ratio, which would be consistent with an increasing emission influence from these basins.

4.6. The Influence of Biomass Burning on Isomeric Ratios

Another possible influence might be exerted by biomass burning emissions. Most types of biomass burning emissions exhibit relatively higher fractions of the *n*-isomers of butane and pentane and have (*i*/*n*) isomeric ratios that are smaller (Table STb2) (Akagi et al., 2011; Andreae & Merlet, 2001) than the average values calculated in our study. The frequency and the area burnt by U.S. wildfires rose from 1984 to 2011 (Dennison et al., 2014). Wildfires are a seasonal emissions source, occurring mostly in the summer, with a trend of increasing seasonal variability from 1995 to 2011 (Zhang et al., 2014). This increase in biomass burning emissions would be expected to result in an increased NMHC source that would drive (*i*/*n*) isomer ratios to lower values. Seven of 10 urban sites had higher (*i*/*n*) pentane isomer ratios in summer months (Table 4). This seasonal signature in the data is expected for OH chemistry, and is the opposite of what would be expected if wildfire emissions exerted a strong summer influence. Therefore, it seems unlikely that increasing biomass burning emissions are exhibiting a determining signature on the data from the urban areas that were considered in this study.

5. Summary and Conclusions

Butane and pentane atmospheric mole fractions, their isomeric ratios, and trends showed a wide range and high variability among sites. A common feature was that average mixing ratios of the butane and pentane isomers have been decreasing at most, that is, 81% of the sites, considered in this study. The exception was SGP, where all four isomers have been increasing (three have a statistically significant trend), most certainly due to increasing O&NG emissions. Similar to individual species, a large range was observed for changes of the (*i*/*n*)

butane and pentane isomeric ratio. All six statistically significant (*i*/*n*) butane trends and all seven statistically significant (*i*/*n*) pentane trends were negative, indicating a relative increase in the prominence of the *n*-isomers.

The most obvious explanation for the observed declines in concentrations and in the (*i*/*n*) isomeric ratio is changes in emission strength and relative contribution from different emission sectors. In the last century, motor vehicle sources have dominated urban emissions of VOC (Parrish et al., 2009; Von Schneidemesser et al., 2010). Clearly, regulations of emission sources have brought mixing ratios of VOC down from their highest levels in the 1970s. Data from our analyses support this previous research, as levels appear to be continuing their decline at most sites evaluated in this work.

The abundance of decreasing (*i*/*n*) pentane ratios, both at urban sites and in the GGGRN, suggests influences on pentane emissions on wide geographical scales. There is a potential contribution from a changing isomeric ratio in gasoline pentanes, but the quantitative contribution from changes in this emission sector cannot be conclusively resolved with the data sets analyzed here. Another possible influence is an increase of the relative contribution of biomass burning emissions. Third, it is notable that decreasing (*i*/*n*) pentane isomeric ratio trends were consistently observed at a site that is heavily influenced, and at sites within relatively close proximity, that is, ~200 miles (~321.9 km), of O&NG development regions. Recent research has shown regionally elevated hydrocarbon concentrations in the United States as a result of O&NG development (Franco et al., 2016; Helmig et al., 2016; Kort et al., 2016; Schade & Roest, 2015 ; Vinciguerra et al., 2015), with pentane isomers constituting on the order of 10% of the total NMHC mass (Helmig et al., 2014). The fact that (*i*/*n*) pentane isomeric ratio trends agree with the expected signature of increasing O&NG influence and the geographic distribution of sites with statistically significant trends of the (*i*/*n*) pentane isomeric ratio and shale plays (Figure 1) suggest an increasing influence of O&NG emissions, regionally and nationwide. This conclusion is in agreement with findings from other recent studies that have shown that O&NG NMHC emissions are constituting an increasing fraction of the urban and rural VOC mix at sites downwind of O&NG basins (Schade & Roest, 2015; Vinciguerra et al., 2015) in the U.S. Similar observations were reported for the United Kingdom: While most C2–C8 hydrocarbons steadily declined from 1993 to 2012, ethane and propane, which are mostly associated to NG emissions, have remained near their 1993 values (Derwent et al., 2017).

Given the relatively wide spread in results, it is difficult to conclude at what exact rate these compounds and their isomeric ratios have changed in the United States as a whole. It is very obvious that multiple sources, exhibiting regionally diverse and different trends, are influencing atmospheric concentrations and isomeric ratios to a variable degree at the considered monitoring sites. Care should be taken utilizing these observations for evaluating emission inventories, as the representativeness of the considered site locations is uncertain. Clearly, there is a need for consideration and comparison of spatially and temporally resolved data for deriving representative estimates on a national scale.

Acknowledgments
We thank all scientists, staff, and agencies who contributed to the collection, posting, and archiving of the PAMS (available at https://www.airnowtech.org/) and GGGRN (available at https://ds.data.jma.go.jp/gmd/wdcgg/) data. We thank the EPA, AirNow-Tech, and the WDCGG for making these data publically available. The VOC observations within the GGGRN are supported in part by the U.S. National Oceanic and Atmospheric Administration's Climate Program Office's AC4 Program. The U.S. National Science Foundation (NSF)–funded project PLR-AON 1108391 supported quality control efforts that benefited the GGGRN data.

References

Akagi, S. K., Yokelson, R. J., Wiedinmyer, C., Alvarado, M. J., Reid, J. S., Karl, T., et al. (2011). Emission factors for open and domestic biomass burning for use in atmospheric models. *Atmospheric Chemistry and Physics*, *11*(9), 4039–4072. https://doi.org/10.5194/acp-11-4039-2011

Andreae, M. O., & Merlet, P. (2001). Emission of trace gases and aerosols from biomass burning. *Global Biogeochemical Cycles*, *15*(4), 955–966. https://doi.org/10.1029/2000GB001382

Atkinson, R. (1997). Gas-phase tropospheric chemistry of volatile organic compounds: 1. Alkanes and alkenes. *Journal of Physical and Chemical Reference Data*, *26*(2), 215–290. https://doi.org/10.1063/1.556012

Atkinson, R. (2000). Atmospheric chemistry of VOCs and NO_x. *Atmospheric Environment*, *34*(12-14), 2063–2101. https://doi.org/10.1016/S1352-2310(99)00460-4

Atkinson, R. (2003). Kinetics of the gas-phase reactions of OH radicals with alkanes and cycloalkanes. *Atmospheric Chemistry and Physics*, *3*(6), 2233–2307. https://doi.org/10.5194/acp-3-2233-2003

Atkinson, R., & Arey, J. (2003). Gas-phase tropospheric chemistry of biogenic volatile organic compounds: A review. *Atmospheric Environment*, *37*, S197–S219.

Atkinson, R., & Carter, W. P. L. (1984). Kinetics and mechanisms of the gas-phase reactions of ozone with organic compounds under atmospheric conditions. *Chemical Reviews*, *84*(5), 437–470. https://doi.org/10.1021/cr00063a002

Atkinson, R., Winer, A. M., & Pitts, J. N. (1986). Estimation of nighttime N_2O_5 concentrations from ambient NO_2 and NO_3 radical concentrations and the role of N_2O_5 in nighttime chemistry. *Atmospheric Environment*, *20*(2), 331–339. https://doi.org/10.1016/0004-6981(86)90035-1

Aydin, M., Verhulst, K. R., Saltzman, E. S., Battle, M. O., Montzka, S. A., Blake, D. R., et al. (2011). Recent decreases in fossil-fuel emissions of ethane and methane derived from firn air. *Nature*, *476*(7359), 198–201. https://doi.org/10.1038/nature10352

Baker, A. K., Rauthe-Schoch, A., Schuck, T. J., Brenninkmeijer, C. A. M., van Velthoven, P. F. J., Wisher, A., & Oram, D. E. (2011). Investigation of chlorine radical chemistry in the Eyjafjallajokull volcanic plume using observed depletions in non-methane hydrocarbons. *Geophysical Research Letters*, *38*, L13801. https://doi.org/10.1029/2011GL047571

Bishop, G. A., & Stedman, D. H. (2008). A decade of on-road emissions measurements. *Environmental Science & Technology*, *42*(5), 1651–1656. https://doi.org/10.1021/es702413b

Blake, N. J., Penkett, S. A., Clemitshaw, K. C., Anwyl, P., Lightman, P., Marsh, A. R. W., & Butcher, G. (1993). Estimates of atmospheric hydroxyl radical concentrations from the observed decay of many reactive hydrocarbons in well-defined urban plumes. *Journal of Geophysical Research*, *98*(D2), 2851–2864. https://doi.org/10.1029/92JD02161

Borner, J., & Wunder, S. (2012). The scope for reducing emissions from forestry and agriculture in the Brazilian Amazon. *Forests*, *3*(4), 546–572. https://doi.org/10.3390/f3030546

Burruss, R. C., & Ryder, R. T. (2014). Composition of natural gas and crude oil produced from 14 wells in the Lower Silurian "Clinton" Sandstone and Medina Group Sandstones, northeastern Ohio and Northwestern Pennsylvania. *U.S. Geological Survey Professional Paper*, *1708*, 38.

Calvert, J. G. (1976). Hydrocarbon involvement in photochemical smog formation in Los Angeles atmosphere. *Environmental Science & Technology*, *10*(3), 256–262. https://doi.org/10.1021/es60114a003

Colon-Roman, Y. A., & Ruppert, L. F. (2014). Central Appalachian basin natural gas database—Distribution, composition, and origin of natural gases. *U.S. Geological Survey Open-File Report*, *2014–1207*, 13.

de Gouw, J. A., Cooper, O. R., Warneke, C., Hudson, P. K., Fehsenfeld, F. C., Holloway, J. S., et al. (2004). Chemical composition of air masses transported from Asia to the U. S. West Coast during ITCT 2K2: Fossil fuel combustion versus biomass-burning signatures. *Journal of Geophysical Research*, *109*, D23S20. https://doi.org/10.1029/2003JD004202

D.E.P., P. D. o. E. P (2017). Oil and gas well production, edited by P. D. o. E. Protection, Pennsylvania Department of Environmental Protection. Retrieved from http://www.depreportingservices.state.pa.us/ReportServer/Pages/ReportViewer.aspx?%2fOil_Gas%2fOil_Gas_Well_Production

Davies, L., & Gather, U. (1993). The identification of multiple outliers. *Journal of the American Statistical Association*, *88*(423), 782–792. https://doi.org/10.1080/01621459.1993.10476339

Demirbas, A. (2010). Methane gas hydrate. In *Methane Gas Hydrate* (pp. 1–186). New York: Springer.

Dennison, P. E., Brewer, S. C., Arnold, J. D., & Moritz, M. A. (2014). Large wildfire trends in the western United States, 1984–2011. *Geophysical Research Letters*, *41*, 2928–2933. https://doi.org/10.1002/2014GL059576

Derwent, R. G., Field, R. A., Dumitrean, P., Murrells, T. P., & Telling, S. P. (2017). Origins and trends in ethane and propane in the United Kingdom from 1993 to 2012. *Atmospheric Environment*, *156*, 15–23. https://doi.org/10.1016/j.atmosenv.2017.02.030

EIA (1998). In D. o. Energy (Ed.), *Refiners Switch to Reformulated Gasoline Complex Model*. Washington, DC: United States Energy Information Administration.

EIA (2017). Shale gas production, natural gas. In *U.S. Energy Information Administration*. Washington, DC: United States Department of Energy.

EPA (1997). In E. P. Agency (Ed.), *Photochemical Assessment Monitoring Stations (PAMS) Performance Evaluation Program*. Morrisville, NC: Office of Air Quality Planning and Standards.

EPA (1998). Technical Assistance Document (TAD) for sampling and analysis of ozone precursors, edited, EPA.

EPA (2006a). *RFG Property and Performance Averages for Baltimore, MD* (1 pp.). Washington, DC: United States Environmental Protection Agency.

EPA (2006b). RFG property and performance averages for Boston-Worchester, MA. In *Fuels and Fuel Additives* (1 pp.). Washington, DC: United States Environmental Protection Agency.

EPA (2006c). RFG property and performance averages for Chicago-Lake Co., IL, Gary, IN. In *Fuels and Fuel Additives* (1 pp.). Washington, DC: United States Environmental Protection Agency.

EPA (2006d). RFG property and performance averages for Houston-Galveston, TX. In *Fuels and Fuel Additives* (1 pp.). Washington, DC: United States Environmental Protection Agency.

EPA (2006e). RFG property and performance averages for Phila.-Wilm, DE-Trenton, NJ. In *Fuels and Fuel Additives* (1 pp.). Washington, DC: United States Environmental Protection Agency.

EPA (2006f). RFG property and performance averages for Springfield, MA. In *Fuels and Fuel Additives*. Washington, DC: United States Environmental Protection Agency.

EPA (2016). US Greenhouse Gas Inventory. Retrieved from https://www3.epa.gov/climatechange/ghgemissions/index.html

EPA (2017). Gasoline Reid vapor pressure. Retrieved from https://www.epa.gov/gasoline-standards/gasoline-reid-vapor-pressure

Faiz, A., Weaver, C. S., & Walsh, M. P. (1996). Air pollution from motor vehicles, edited by T. I. Bank, Library of Congress cataloging-in-publication data Reconstruction and Development/ The World Bank.

Franco, B., Mahieu, E., Emmons, L. K., Tzompa-Sosa, Z. A., Fischer, E. V., Sudo, K., et al. (2016). Evaluating ethane and methane emissions associated with the development of oil and natural gas extraction in North America. *Environmental Research Letters*, *11*(4), 1–11. https://doi.org/10.1088/1748-9326/11/4/044010

Fujita, E. M., Croes, B. E., Bennett, C. L., Lawson, D. R., Lurmann, F. W., & Main, H. H. (1992). Comparison of emission inventory and ambient concentration ratios of CO, NMOG, and NO_x in California's South Coast Air Basin. *Journal of the Air & Waste Management Association*, *42*(3), 264–276. https://doi.org/10.1080/10473289.1992.10466989

Garratt, J. R. (1992). *The Atmospheric Boundary Layer/J. R. Garratt*. Cambridge, New York: Cambridge University Press.

Gilman, J. B., Lerner, B. M., Kuster, W. C., & de Gouw, J. A. (2013). Source signature of volatile organic compounds from oil and natural gas operations in northeastern Colorado. *Environmental Science & Technology*, *47*(3), 1297–1305. https://doi.org/10.1021/es304119a

Goldan, P. D., Kuster, W. C., Fehsenfeld, F. C., & Montzka, S. A. (1995). Hydrocarbon measurements in the southeastern United States: The Rural Oxidants in the Southern Environment (ROSE) program 1990. *Journal of Geophysical Research*, *100*(D12), 25,945–25,963. https://doi.org/10.1029/95JD02607

Goldstein, A. H., Wofsy, S. C., & Spivakovsky, C. M. (1995). Seasonal variations of nonmethane hydrocarbons in rural New England: Constraints on OH concentrations in northern midlatitudes (vol 100, pg 21023, 1995). *Journal of Geophysical Research*, *100*(D12), 26,273–26,274. https://doi.org/10.1029/95JD03428

Hatch, S. A. (2003). Statistical power for detecting trends with applications to seabird monitoring. *Biological Conservation*, *111*(3), 317–329. https://doi.org/10.1016/S0006-3207(02)00301-4

Helmig, D., Tanner, D. M., Honrath, R. E., Owen, R. C., & Parrish, D. D. (2008). Nonmethane hydrocarbons at Pico Mountain, Azores: 1. Oxidation chemistry in the North Atlantic region. *Journal of Geophysical Research*, *113*, D20S91. https://doi.org/10.1029/2007JD008930

Helmig, D., Stephens, C. R., Caramore, J., & Hueber, J. (2014). Seasonal behavior of non-methane hydrocarbons in the firn air at Summit, Greenland. *Atmospheric Environment*, *85*, 234–246.

Helmig, D., Thompson, C. R., Evans, J., Boylan, P., Hueber, J., & Park, J. H. (2014). Highly elevated atmospheric levels of volatile organic compounds in the Uintah Basin, Utah. *Environmental Science & Technology*, *48*(9), 4707–4715.

Helmig, D., Muñoz, M., Hueber, J., Mazzoleni, C., Mazzoleni, L., Owen, R. C., et al. (2015). Climatology and atmospheric chemistry of the non-methane hydrocarbons ethane and propane over the North Atlantic. *Elementa-Science of the Anthropocene*, *3*, 1–16.

Helmig, D., Rossabi, S., Hueber, J., Tans, P., Montzka, S. A., Masarie, K., et al. (2016). Reversal of global atmospheric ethane and propane trends largely due to U.S. oil and natural gas production. *Nature Geoscience*, *9*(7), 490–495. https://doi.org/10.1038/ngeo2721

Hirsch, R. M., Alexander, R. B., & Smith, R. A. (1991). Selection of methods for the detection and estimation of trends in water-quality. *Water Resources Research*, *27*(5), 803–813. https://doi.org/10.1029/91WR00259

Honrath, R. E., Helmig, D., Owen, R. C., Parrish, D. D., & Tanner, D. M. (2008). Nonmethane hydrocarbons at Pico Mountain, Azores: 2. Event-specific analyses of the impacts of mixing and photochemistry on hydrocarbon ratios. *Journal of Geophysical Research*, *113*, D20S92. https://doi.org/10.1029/2008JD009832

Hornbrook, R. S., Hills, A. J., Riemer, D. D., Abdelhamid, A., Flocke, F. M., Hall, S. R., et al. (2016). Arctic springtime observations of volatile organic compounds during the OASIS-2009 campaign. *Journal of Geophysical Research*, *121*, 9789–9813. https://doi.org/10.1002/2015JD024360

Isaksen, I. S. A., Hov, O., Penkett, S. A., & Semb, A. (1985). Model analysis of the measured concentration of organic gases in the Norwegian Arctic. *Journal of Atmospheric Chemistry*, *3*(1), 3–27. https://doi.org/10.1007/BF00049366

Jobson, B. T., Niki, H., Yokouchi, Y., Bottenheim, J., Hopper, F., & Leaitch, R. (1994). Measurements of C-2-C-6 hydrocarbons during the polar sunrise 1992 experiment—Evidence of Cl atom and Br atom chemistry. *Journal of Geophysical Research*, *99*(D12), 25,355–25,368. https://doi.org/10.1029/94JD01243

Jobson, B. T., Wu, Z., Niki, H., & Barrie, L. A. (1994). Seasonal trends of isoprene, C-2-C-5 alkanes, and acetylene at a remote boreal site in Canada. *Journal of Geophysical Research*, *99*(D1), 1589–1599. https://doi.org/10.1029/93JD00424

Jobson, B. T., Berkowitz, C. M., Kuster, W. C., Goldan, P. D., Williams, E. J., Fesenfeld, F. C., et al. (2004). Hydrocarbon source signatures in Houston, Texas: Influence of the petrochemical industry. *Journal of Geophysical Research*, *109*, D24305. https://doi.org/10.1029/2004JD004887

Kasting, J. F., & Singh, H. B. (1986). Nonmethane hydrocarbons in the troposphere—Impact on the odd hydrogen and odd nitrogen chemistry. *Journal of Geophysical Research*, *91*(D12), 3239–3256.

Kendall, M. G. (1975). *Rank Correlation Methods* (4th ed.). London: Charles Griffin.

Kort, E. A., Smith, M. L., Murray, L. T., Gvakharia, A., Brandt, A. R., Peischl, J., et al. (2016). Fugitive emissions from the Bakken shale illustrate role of shale production in global ethane shift. *Geophysical Research Letters*, *43*, 4617–4623. https://doi.org/10.1002/2016GL068703

Krohn, J., & Nulle, G. (2015). Utica provides 85% of U.S. shale gas production growth since start of 2012, edited, U.S. Energy Information Administration.

Lacey, W. N., Sage, B. H., & Kircher, C. E. (1934). Phase equilibria in hydrocarbon systems: III. Solubility of a dry natural gas in crude oil. *Industrial and Engineering Chemistry*, *26*(6), 652–654. https://doi.org/10.1021/ie50294a014

LaFranchi, B. W., Pétron, G., Miller, J. B., Lehman, S. J., Andrews, A. E., Dlugokencky, E. J., et al. (2013). Constraints on emissions of carbon monoxide, methane, and a suite of hydrocarbons in the Colorado Front Range using observations of (CO2)-C-14. *Atmospheric Chemistry and Physics*, *13*(21), 11,101–11,120. https://doi.org/10.5194/acp-13-11101-2013

Lewis, A. C., Evans, M. J., Hopkins, J. R., Punjabi, S., Read, K. A., Purvis, R. M., et al. (2013). The influence of biomass burning on the global distribution of selected non-methane organic compounds. *Atmospheric Chemistry and Physics*, *13*(2), 851–867. https://doi.org/10.5194/acp-13-851-2013

Liu, S. C., Trainer, M., Fehsenfeld, F. C., Parrish, D. D., Williams, E. J., Fahey, D. W., et al. (1987). Ozone production in the rural troposphere and the implications for regional and global ozone distributions. *Journal of Geophysical Research*, *92*(D4), 4191–4207. https://doi.org/10.1029/JD092iD04p04191

Mann, H. B. (1945). Nonparametric tests against trend. *Econometrica*, *13*(3), 245–259. https://doi.org/10.2307/1907187

Mayrsohn, H., & Crabtree, J. H. (1976). Source reconciliation of atmospheric hydrocarbons. *Atmospheric Environment*, *10*(2), 137–143. https://doi.org/10.1016/0004-6981(76)90231-6

McDonald, B. C., Gentner, D. R., Goldstein, A. H., & Harley, R. A. (2013). Long-term trends in motor vehicle emissions in US urban areas. *Environmental Science & Technology*, *47*(17), 10,022–10,031. https://doi.org/10.1021/es401034z

McKeen, S. A., & Liu, S. C. (1993). Hydrocarbon ratios and photochemical histories of air masses. *Geophysical Research Letters*, *20*(21), 2363–2366. https://doi.org/10.1029/93GL02527

Monks, P. S., Granier, C., Fuzzi, S., Stohl, A., Williams, M. L., Akimoto, H., et al. (2009). Atmospheric composition change—Global and regional air quality. *Atmospheric Environment*, *43*(33), 5268–5350. https://doi.org/10.1016/j.atmosenv.2009.08.021

Parrish, D. D., Hahn, C. J., Williams, E. J., Norton, R. B., Fehsenfeld, F. C., Singh, H. B., et al. (1992). Indications of photochemical histories of Pacific air masses from measurements of atmospheric trace species at Point Arena, California. *Journal of Geophysical Research*, *97*(D14), 15,883–15,901. https://doi.org/10.1029/92JD01242

Parrish, D. D., Trainer, M., Young, V., Goldan, P. D., Kuster, W. C., Jobson, B. T., et al. (1998). Internal consistency tests for evaluation of measurements of anthropogenic hydrocarbons in the troposphere. *Journal of Geophysical Research*, *103*(D17), 22,339–22,359. https://doi.org/10.1029/98JD01364

Parrish, D. D., Kuster, W. C., Shao, M., Yokouchi, Y., Kondo, Y., Goldan, P. D., et al. (2009). Comparison of air pollutant emissions among mega-cities. *Atmospheric Environment*, *43*(40), 6435–6441. https://doi.org/10.1016/j.atmosenv.2009.06.024

Pearson, R. K., Neuvo, Y., Astola, J., Gabbouj, M., & IEEE (2015). The class of generalized Hampel filters. In *2015 23rd European Signal Processing Conference* (pp. 2501–2505). New York: IEEE.

Peischl, J., Ryerson, T. B., Brioude, J., Aikin, K. C., Andrews, A. E., Atlas, E., et al. (2013). Quantifying sources of methane using light alkanes in the Los Angeles basin, California. *Journal of Geophysical Research: Atmospheres*, *118*, 4974–4990. https://doi.org/10.1002/jgrd.50413

Penkett, S. A., Blake, N. J., Lightman, P., Marsh, A. R. W., Anwyl, P., & Butcher, G. (1993). The seasonal-variation of nonmethane hydrocarbons in the free troposphere over the North-Atlantic Ocean—Possible evidence for extensive reaction of hydrocarbons with the nitrate radical. *Journal of Geophysical Research*, *98*(D2), 2865–2885. https://doi.org/10.1029/92JD02162

Pétron, G., Frost, G., Miller, B. R., Hirsch, A. I., Montzka, S. A., Karion, A., et al. (2012). Hydrocarbon emissions characterization in the Colorado Front Range: A pilot study. *Journal of Geophysical Research*, *117*, D04304. https://doi.org/10.1029/2011JD016360

Pierson, W. R., Schorran, D. E., Fujita, E. M., Sagebiel, J. C., Lawson, D. R., & Tanner, R. L. (1999). Assessment of nontailpipe hydrocarbon emissions from motor vehicles. *Journal of the Air & Waste Management Association*, *49*(5), 498–519. https://doi.org/10.1080/10473289.1999.10463827

Platt, U., Perner, D., Winer, A. M., Harris, G. W., & Pitts, J. N. (1980). Detection of NO_3 in the polluted troposphere by differential optical absorption. *Geophysical Research Letters*, *7*(1), 89–92. https://doi.org/10.1029/GL007i001p00089

Pollmann, J., Helmig, D., Hueber, J., Plass-Dülmer, C., & Tans, P. (2008). Sampling, storage, and analysis of C2-C7 non-methane hydrocarbons from the US National Oceanic and Atmospheric Administration Cooperative Air Sampling Network glass flasks. *Journal of Chromatography A*, *1188*(2), 75–87. https://doi.org/10.1016/j.chroma.2008.02.059

Pollmann, J., Helmig, D., Liptzin, D., Thompson, C. R., Hueber, J., & Tans, P. (2016). Variability analyses, site characterization, and regional [OH] estimates using trace gas measurements from NOAA Global Greenhouse Gas Reference Network. *Elementa-Science of the Anthropocene*, *4*(128), 1–14.

Roberts, J. M., Fehsenfeld, F. C., Liu, S. C., Bollinger, M. J., Hahn, C., Albritton, D. L., & Sievers, R. E. (1984). Measurements of aromatic hydrocarbon ratios and NO_x concentrations in the rural troposphere—Observation of air-mass photochemical aging and NO_x removal. *Atmospheric Environment*, *18*(11), 2421–2432. https://doi.org/10.1016/0004-6981(84)90012-X

Rudolph, J., & Ehhalt, D. H. (1981). Measurements of C2–C5 Hydrocarbons over the North Atlantic. *Journal of Geophysical Research*, *86*(NC12), 1959–1964.

Schade, G. W., & Roest, G. S. (2015). Is the shale boom reversing progress in curbing ozone pollution? *Eos*, *96*. https://doi.org/10.1029/2015EO028279

Scheff, P. A., Wadden, R. A., Kenski, D. M., Chung, J., & Wolff, G. (1996). Receptor model evaluation of the southeast Michigan ozone study ambient NMOC measurements. *Journal of the Air & Waste Management Association*, *46*(11), 1048–1057. https://doi.org/10.1080/10473289.1996.10467540

Seidel, D. J., Zhang, Y., Beljaars, A., Golaz, J.-C., Jacobson, A. R., & Medeiros, B. (2012). Climatology of the planetary boundary layer over the continental United States and Europe. *Journal of Geophysical Research*, *117*, D17106. https://doi.org/10.1029/2012JD018143

Sen, P. K. (1968). Estimates of regression coefficient based on Kendall's tau. *Journal of the American Statistical Association*, *63*(324), 1379.

Singh, H., & Zimmerman, P. B. (1992). Atmospheric distribution and sources of nonmethane hydrocarbons. *Advances in Environmental Science & Technology*, *24*, 177–235.

Stull, R. B. (1988). *An Intoduction to Boundary Layer Meteorology* (Vol. 1, p. 670). Dordrecht, Netherlands: Springer.

Swarthout, R. F., Russo, R. S., Zhou, Y., Hart, A. H., & Sive, B. C. (2013). Volatile organic compound distributions during the NACHTT campaign at the Boulder Atmospheric Observatory: Influence of urban and natural gas sources. *Journal of Geophysical Research*, *118*, 10,614–10,637. https://doi.org/10.1002/jgrd.50722

Swarthout, R. F., Russo, R. S., Zhou, Y., Miller, B. M., Mitchell, B., Horsman, E., et al. (2015). Impact of Marcellus shale natural gas development in Southwest Pennsylvania on volatile organic compound emissions and regional air quality. *Environmental Science & Technology*, *49*(5), 3175–3184.

Theil, H. (1950). A rank invariant method of linear and polynomial regression analysis, *Nederl. Akad. Wetensch., Proc. 53*(I, II, III), 386-392, 521-525,1397-1412.

Thompson, C. R., Hueber, J., & Helmig, D. (2014). Influence of oil and gas emissions on ambient atmospheric non-methane hydrocarbons in residential areas of Northeastern Colorado. *Elementa-Science of the Anthropocene*, *3*(35), 4707–4715.

Thoning, K. W., Tans, P. P., & Komhyr, W. D. (1989). Atmospheric carbon-dioxide at Mauna Loa observatory .2. analysis of the NOAA GMCC data, 1974–1985. *Journal of Geophysical Research*, *94*(D6), 8549–8565.

Trainer, M., Hsie, E. Y., McKeen, S. A., Tallamraju, R., Parrish, D. D., Fehsenfeld, F. C., & Liu, S. C. (1987). Impact of natural hydrocarbons on hydroxy and peroxy-radicals at a remote site. *Journal of Geophysical Research*, *92*(D10), 11,879–11,894. https://doi.org/10.1029/JD092iD10p11879

Vinciguerra, T., Yao, S., Dadzie, J., Chittams, A., Deskins, T., Ehrman, S., & Dickerson, R. R. (2015). Regional air quality impacts of hydraulic fracturing and shale natural gas activity: Evidence from ambient VOC observations. *Atmospheric Environment*, *110*, 144–150. https://doi.org/10.1016/j.atmosenv.2015.03.056

Von Schneidemesser, E., Monks, P. S., & Plass-Duelmer, C. (2010). Global comparison of VOC and CO observations in urban areas. *Atmospheric Environment*, *44*(39), 5053–5064. https://doi.org/10.1016/j.atmosenv.2010.09.010

Warneke, C., de Gouw, J. A., Holloway, J. S., Peischl, J., Ryerson, T. B., Atlas, E., et al. (2012). Multiyear trends in volatile organic compounds in Los Angeles, California: Five decades of decreasing emissions. *Journal of Geophysical Research*, *117*, D00V17. https://doi.org/10.1029/2012JD017899

Wayne, R. P., Barnes, I., Biggs, P., Burrows, J. P., Canosa-Mas, C. E., Hjorth, J., et al. (1991). The nitrate radical: Physics, chemistry, and the atmosphere. *Atmospheric Environment. Part A. General Topics*, *25*(1), 1–203. https://doi.org/10.1016/0960-1686(91)90192-A

Wells, J. (2005). Special gasoline blends reduce emissions and improve air quality, but complicate supply and contribute to higher prices. *Government Accountability Office*, *05*(421), 1–47.

Wilson, E. W., Hamilton, W. A., Kennington, H. R., Evans, B., Scott, N. W., & DeMore, W. B. (2006). Measurement and estimation of rate constants for the reactions of hydroxyl radical with several alkanes and cycloalkanes. *The Journal of Physical Chemistry. A*, *110*(10), 3593–3604. https://doi.org/10.1021/jp055841c

World Meteorological Organization (1995). *Scientific Assessment of Ozone Depletion: World Meterological Organization Global Ozone Research and Monitoring Project*, *Report No. 37*, Geneva, Switzerland, 1994, February, 1995.

Worton, D. R., Sturges, W. T., Reeves, C. E., Newland, M. J., Penkett, S. A., Atlas, E., et al. (2012). Evidence from firn air for recent decreases in non-methane hydrocarbons and a 20th century increase in nitrogen oxides in the northern hemisphere. *Atmospheric Environment*, *54*, 592–602. https://doi.org/10.1016/j.atmosenv.2012.02.084

Zhang, X. Y., Kondragunta, S., & Roy, D. P. (2014). Interannual variation in biomass burning and fire seasonality derived from geostationary satellite data across the contiguous United States from 1995 to 2011. *Journal of Geophysical Research: Biogeosciences*, *119*, 1147–1162. https://doi.org/10.1002/2013JG002518